Article

# Metal Atoms Collinear with the Spiro Carbon of 6,6-Open Adducts, M@C(Ad) (M = La and Ce, Ad = Adamantylidene)

Michio Yamada, Chika Someya, Takatsugu Wakahara, Takahiro Tsuchiya, Yutaka Maeda, Takeshi Akasaka, Kenji Yoza, Ernst Horn, Michael T. H. Liu, Naomi Mizorogi, and Shigeru Nagase

*J. Am. Chem. Soc.*, **2008**, 130 (4), 1171-1176 • DOI: 10.1021/ja073924w



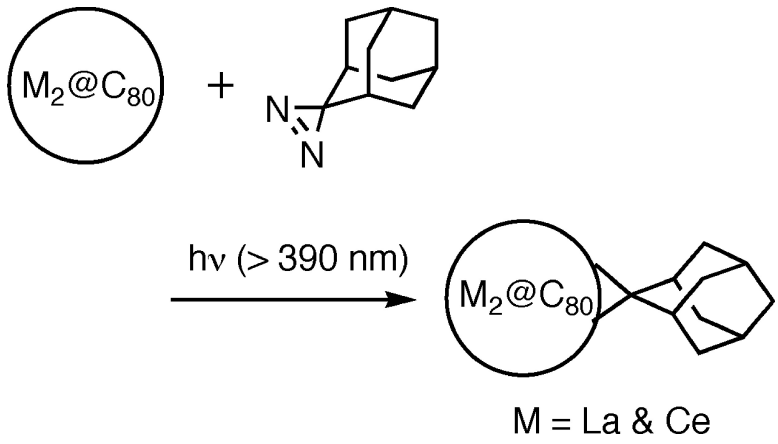


## More About This Article

Additional resources and features associated with this article are available within the HTML version:

- Supporting Information
- Links to the 4 articles that cite this article, as of the time of this article download
- Access to high resolution figures
- Links to articles and content related to this article
- Copyright permission to reproduce figures and/or text from this article

View the Full Text HTML

J|A|C|S
ARTICLES
Published on Web 01/08/2008

# Metal Atoms Collinear with the Spiro Carbon of 6,6-Open Adducts, $M_2@C_{80}$(Ad) (M = La and Ce, Ad = Adamantylidene)

Michio Yamada,[†] Chika Someya,[†] Takatsugu Wakahara,[†] Takahiro Tsuchiya,[†] Yutaka Maeda,[‡] Takeshi Akasaka,*[,†] Kenji Yoza,[§] Ernst Horn,[⊥] Michael T. H. Liu,[○] Naomi Mizorogi,[#] and Shigeru Nagase*[,#]

*Center for Tsukuba Advanced Research Alliance, University of Tsukuba, Tsukuba, Ibaraki 305-8577, Japan, Department of Chemistry, Tokyo Gakugei University, Koganei, Tokyo 184-8501, Japan, Bruker AXS, K. K., Yokohama, Kanagawa 221-0022, Japan, Department of Chemistry, Rikkyo University, Tokyo 171-8501, Japan, University of Prince Edward Island, Charlottetown, Prince Edward Island, Canada C1A4P3, and Department of Theoretical and Computational Molecular Science, Institute for Molecular Science, Okazaki, Aichi 444-8585, Japan*

Received May 31, 2007; E-mail: akasaka@tara.tsukuba.ac.jp

***Abstract:*** The photochemical reaction of $M_2@C_{80}$ (M = La and Ce) with 2-adamantane-2,3′-[3H]-diazirine (**1**) affords the corresponding adducts by carbene addition. The adducts were characterized by spectroscopic and single-crystal X-ray structure analyses. Crystallographic data for the adduct $La_2@C_{80}$(Ad) (**2**, Ad = adamantylidene) reveal that the two La atoms are collinear with the spiro carbon of the 6,6-open adduct. It is noteworthy that the La−La distance is highly elongated by the addition of carbene. Paramagnetic $^{13}C$ NMR spectral analysis of the adduct $Ce_2@C_{80}$(Ad) (**3**) indicates that the two Ce atoms are also collinear with the spiro carbon at room temperature in solution. The unique metal positions were confirmed by density functional calculations.

## Introduction

Endohedral metallofullerenes present unique structures and properties because the encapsulated metal atom(s) can donate electrons to the fullerene cages.[1] Recent progress on the isolation and purification of endohedral metallofullerenes in macroscopic quantities have made it possible to investigate their interesting electronic properties and reactivities.[2] Among many kinds of endohedral metallofullerenes, $La_2@C_{80}$ has attracted special attention because of the three-dimensional random motion of two La atoms inside the $C_{80}$ cage.[3] It is instructive to note that the small rotational barrier in $La_2@C_{80}$ originates from the round $I_h$ $C_{80}$ cage and the electronic structure formally described as $(La^{3+})_2C_{80}^{6-}$.[3a,4] The positively charged La atoms should be highly stabilized at the minimum of electrostatic potentials inside $C_{80}^{6-}$. However, the electrostatic potential map shows almost concentric circles around the center of $C_{80}$, because of the round $I_h$ cage. For this reason,[4] the $La^{3+}$ ion is not highly stabilized at specific bonding sites. Recently, similar interesting systems with the $I_h$ $C_{80}$ cage, $M_3N@C_{80}$ (M = Sc and Y), have also been investigated.[5] Control of such motion of atoms within a cage is expected to be very valuable in designing functional molecular devices with new electronic or magnetic properties.[6]

In 2005, we reported the synthesis and characterization of an exohedrally silylated derivative, $Ce_2@C_{80}(Mes_2Si)_2CH_2$ (Mes = mesityl),[7] as an analogue of $La_2@C_{80}$. Two encapsulated Ce atoms are localized inside the silylated $C_{80}$ cage, according to X-ray crystallographic and $^{13}C$ NMR spectroscopic analyses. X-ray crystallographic analysis of the silylated $Ce_2@C_{80}$ clearly showed that the two Ce atoms are localized at two positions directing the hexagonal ring at the equator. In addition, very recently we have also reported the synthesis and characterization of the exohedrally silylated derivative of $La_2@C_{80}$, $La_2@C_{80}(Ar_2Si)_2CH_2$ (Ar = Mes and Dep, Dep = 2,6-diethylphenyl), and revealed that the two La atoms hop two-dimensionally along the equator of the $C_{80}$ cage.[8] These results indicate that exohedral chemical functionalization of the fullerene surface can regulate the motion of the encapsulated metal atoms drastically.

[†] University of Tsukuba.
[‡] Tokyo Gakugei University.
[§] Bruker AXS K. K.
[⊥] Rikkyo University.
[○] University of Prince Edward Island.
[#] Institute for Molecular Science.

(1) *Endofullerenes: A New Family of Carbon Clusters*; Akasaka, T., Nagase, S., Eds.; Kluwer: Dordrecht, The Netherlands, 2002.
(2) (a) Tsuchiya, T.; Wakahara, T.; Shirakura, S.; Maeda, Y.; Akasaka, T.; Kobayashi, K.; Nagase, S.; Kato, T.; Kadish, K. M. *Chem. Mater.* **2004**, *16*, 4343−4346. (b) Tsuchiya, T.; Wakahara, T.; Lian, Y.; Maeda, Y.; Akasaka, T.; Kato, T.; Mizorogi, N.; Nagase, S. *J. Phys. Chem. B* **2006**, *110*, 22157−22520.
(3) (a) Kobayashi, K.; Nagase, S.; Akasaka, T.; *Chem. Phys. Lett.* **1996**, *261*, 502−506. (b) Akasaka, T.; Nagase, S.; Kobayashi, K.; Waelchli, M.; Yamamoto, K.; Funasaka, H.; Kako, M.; Hoshino, T.; Erata, T. *Angew. Chem., Int. Ed. Engl.* **1997**, *36*, 1643−1645. (c) Nishibori, E.; Takata, M.; Sakata, M.; Taninaka, A.; Shinohara, H. *Angew. Chem., Int. Ed.* **2001**, *40*, 2998−2999. (d) Shimotani, H.; Ito, T.; Iwasa, Y.; Taninaka, A.; Shinohara, H.; Nishibori, E.; Takata, M.; Sakata. M. *J. Am. Chem. Soc.* **2004**, *126*, 364−369.
(4) (a) Kobayashi, K.; Nagase, S.; Akasaka, T. *Chem. Phys. Lett.* **1995**, *245*, 230−236. (b) Kobayashi, K.; Nagase, S. *Chem. Phys. Lett.* **1996**, *262*, 227−232.

It is very interesting to know what dominates the dynamic behavior of the encapsulated metal atoms. In 2006, we reported the synthesis and characterization of two regioisomers of endohedral pyrrolidinodimetallofullerene, $La_2@C_{80}(CH_2)_2NTrt$ (Trt = triphenylmethyl).[9] X-ray crystallographic analysis of the 6,6-adduct of $La_2@C_{80}(CH_2)_2NTrt$, named 6,6- $La_2@C_{80}(CH_2)_2$-NTrt, shows that the two La atoms are localized at the slanted position. The electrostatic potential map calculated inside $[6,6\text{-}C_{80}(CH_2)_2NH]^{6-}$ shows a minimum at the slanted position on the mirror plane inside the cage. The minimum position is in good agreement with the metal position observed in the X-ray crystallographic data. Therefore it is suggested that the metal position inside the functionalized fullerene cage corresponds to the energy minimum on the electrostatic potentials. For the 5,6-adduct, the electrostatic potentials inside the cage are flat and suggest that two La atoms can rotate rather freely. These results indicate that the motion of metal atoms is controllable by the addition positions of the addends. From the viewpoint of designing functional molecular devices, it is important to regulate the metal position to the desirable one inside the cage.

In this article we report that the selective addition of the adamantylidene carbene generated by photoirradiation to 2-adamantane-2,3′-[3H]-diazirine (**1**) occurs at the 6,6-junction of the $M_2@C_{80}$ to afford the formation of $M_2@C_{80}$(Ad) (**2**: M = La, **3**: M = Ce, Ad = adamantylidene) by opening the 6,6-junction. Furthermore, the unique structures of **2** and **3** are also discussed.

## Experimental Section

**General.** Toluene was distilled over benzophenone sodium ketyl under an argon atmosphere prior to use for the reactions. 1,2-Dichlorobenzene (ODCB) was distilled over $P_2O_5$ under vacuum prior to use. $CS_2$ was distilled over $P_2O_5$ under an argon atmosphere prior to use. HPLC isolation was performed on an LC-908 (Japan Analytical Industry Co., Ltd.) monitored by UV absorption at 330 nm. Toluene was used as the eluent. Mass spectroscopy was performed on a Bruker BIFLEX III with 1,1,4,4-tetraphenyl-1,3-butadiene as matrix. The vis−near-IR absorption spectra were measured in $CS_2$ solution by using a SHIMADZU UV-3150 spectrophotometer. Cyclic voltammograms (CVs) and differential pulse voltammograms (DPVs) were recorded on a BAS CV50W electrochemical analyzer. Platinum wires were used as the working electrode and the counter electrode, respectively. The reference electrode was a saturated calomel reference electrode (SCE) filled with 0.1 M $(n\text{-}Bu)_4NPF_6$ in ODCB. All potentials are referenced to the ferrocene/ferrocenium couple ($Fc/Fc^+$) as the standard. CV: scan rate, 20 mV/s. DPV: pulse amplitude, 50 mV; pulse width, 50 ms; pulse period, 200 ms; scan rate, 20 mV/s. NMR spectra were obtained with a Bruker AVANCE-500 with a CryoProbe system.

**Preparation and Purification of $M_2@C_{80}$ (M = La and Ce).** The soot containing lanthanide metallofullerenes were prepared according to the reported procedure using a composite anode which contains graphite and the metal oxide with the atomic ratio of M/C equal to 2.0%.[10] The composite rod was subjected to an arc discharge as an anode under a 150 Torr He pressure. The raw soot containing lanthanide metallofullerenes was collected and extracted with 1,2,4-trichlorobenzene (TCB) solvent for 15 h. The soluble fraction was injected into the HPLC; a 5PYE column (20 mm × 250 mm i.d.; Cosmosil, Nacalai Tesque, Inc.) was used in the first step and a Buckyprep column (20 mm × 250 mm i.d.; Cosmosil, Nacalai Tesque, Inc.) in the second step to give pure $M_2@C_{80}$.

**Preparation and Purification of $^{13}C$-Enriched $Ce_2@C_{80}$.** The soot containing $^{13}C$-enriched cerium metallofullerenes was prepared by the DC arc discharge method under a 300 Torr He pressure. Mixtures of $CeNi_2$ powder and $^{13}C$-graphite powder were pressed into the hole (4.5 mm × 120 mm i.d.) of $^{12}C$-graphite rod (6.3 mm × 130 mm i.d.) in a molecular $CeNi_2/^{13}C$ ratio of 1:10 as an anode. The raw soot containing $^{13}C$-enriched cerium metallofullerenes was collected and extracted with TCB solvent for 15 h. The soluble fraction was injected into the HPLC; a 5PYE column was used in the first step and a Buckyprep column in the second step to give 14% $^{13}C$-enriched $Ce_2@C_{80}$.

**Photochemical Reaction of $La_2@C_{80}$ with 1.** A 19 mL aliquot of a toluene solution of $La_2@C_{80}$ (1.0 mg, $8.1 \times 10^{-7}$ mol) and **1** (26 mg, $1.6 \times 10^{-4}$ mol) was placed in a Pyrex tube, degassed by freeze−pump−thaw cycles under reduced pressures and then irradiated with a high-pressure mercury-arc lamp (cutoff <390 nm) for 9 min. The adduct **2** was easily isolated from the unreacted **1** and $La_2@C_{80}$ by preparative HPLC using a Buckyprep column.

**Photochemical Reaction of $Ce_2@C_{80}$ with 1.** A 19 mL aliquot of a toluene solution of $Ce_2@C_{80}$ (1.0 mg, $8.1 \times 10^{-7}$ mol) and **1** (26 mg, $1.6 \times 10^{-4}$ mol) was placed in a Pyrex tube, degassed by freeze−pump−thaw cycles under reduced pressures, and then irradiated with a high-pressure mercury-arc lamp (cutoff <390 nm) for 9 min. The adduct **3** was easily isolated from the unreacted **1** and $Ce_2@C_{80}$ by preparative HPLC using a Buckyprep column.

**$La_2@C_{80}$(Ad) (2):** $^1H$ NMR (500 MHz, $C_2D_2Cl_4/CS_2$, 303 K) $\delta$ 2.34 (brd, 2H), 2.45 (brs, 1H), 2.47 (brd, $J$ = 15 Hz, 2H), 2.55 (brd, $J$ = 11 Hz, 2H), 2.66 (brs, 1H), 2.88 (brd, $J$ = 12 Hz, 2H), 3.49 (brd, $J$ = 15

(5) (a) Stevenson, S.; Rice, G.; Glass, T.; Harich, K.; Cromer, F.; Jordan, M. R.; Craft, J.; Hadju, E.; Bible, R.; Olmstead, M. M.; Maltra, K.; Fisher, A. J.; Balch, A. L.; Dorn, H. C. *Nature* **1999**, *401*, 55−57. (b) Lezzi, E. B.; Duchamp, J. C.; Harich, K.; Glass, T. E.; Lee, H. M.; Olmstead, M. M.; Balch, A. L.; Dorn, H. C. *J. Am. Chem. Soc.* **2002**, *124*, 524−525. (c) Lee, H. M.; Olmstead, M. M.; Lezzi, E.; Duchamp, J. C.; Dorn, H. C.; Balch, A. L. *J. Am. Chem. Soc.* **2002**, *124*, 3494−3495. (d) Stevenson, S.; Lee, H. M.; Olmstead, M. M.; Kozikowski, C.; Stevenson, P.; Balch, A. L.; *Chem.—Eur. J.* **2002**, *8*, 4528−4535. (e) Stevenson, S.; Phillips, J. P.; Reid, J. E.; Olmstead, M. M.; Rath, S. P.; Balch, A. L. *Chem. Commun.* **2004**, 2814−2815. (f) Cardona, C. M.; Kitaygorodskiy, A.; Ortiz, A.; Herranz, M. A.; Echegoyen, L. *J. Org. Chem.* **2005**, *11*, 3375−3388. (g) Cardona, C. M.; Kitaygorodskiy, A.; Echegoyen, L. *J. Am. Chem. Soc.* **2005**, *127*, 10448−10453. (h) Elliot, B.; Yu, L.; Echegoyen, L. *J. Am. Chem. Soc.* **2005**, *127*, 10885−10888. (i) Cai, T.; Ge, Z.; Lezzi, E. B.; Glass, T. E.; Harich, K.; Gibson, H. W.; Dorn, H. C. *Chem. Commun.* **2005**, 3594−3596. (j) Krause, M.; Liu, X.; Wong, J.; Picher, T.; Knupfer, M.; Dunsch, L. *J. Phys. Chem. A* **2005**, *109*, 7088−7093. (k) Cardona, C. M.; Elliott, B.; Echegoyen, L. *J. Am. Chem. Soc.* **2006**, *128*, 6480−6485. (l) Cai, T.; Slebodnick, C.; Xu, L.; Harich, K.; Glass, T. E.; Chancellor, C.; Fettinger, J. C.; Olmstead, M. M.; Balch, A. L.; Gibson, H. W.; Dorn, H. C. *J. Am. Chem. Soc.* **2006**, *128*, 6486−6492. (m) Cai, T.; Xu, L.; Anderson, M. R.; Ge, Z.; Zuo, T.; Wang, X.; Olmstead, M. M.; Balch, A. L.; Gison, H. W.; Dorn, H. C. *J. Am. Chem. Soc.* **2006**, *128*, 8581−8589. (n) Wang, X.; Zuo, T.; Olmstead, M. M.; Duchamp, J. C.; Glass, T. E.; Cromer, F.; Balch, A. L.; Dorn, H. C. *J. Am. Chem. Soc.* **2006**, *128*, 8884−8889. (o) Wakahara, T.; Iiduka, Y.; Ikenaga, O.; Nakahodo, T.; Sakuraba, A.; Tsuchiya, T.; Maeda, Y.; Kako, M.; Akasaka, T.; Yoza, K.; Horn, E.; Mizorogi, N.; Nagase, S. *J. Am. Chem. Soc.* **2006**, *128*, 9919−9925. (p) Yang, S.; Troyanov, S. I.; Popov, A. A.; Krause, M.; Dunsch, L. *J. Am. Chem. Soc.* **2006**, *128*, 16733−16739. (q) Echegoyen, L.; Chancellor, C. J.; Cardona, C. M.; Elliott, B.; Rivera, J.; Olmstead, M. M.; Balch, A. L. *Chem. Commun.* **2006**, 2653−2655. (r) Martin, N.; Altable, M.; Filippone, S.; Martin-Domenech, A.; Echegoyen, L.; Cardona, C. M. *Angew. Chem., Int. Ed.* **2006**, *45*, 110−114. (s) Lukoyanova, O.; Cardona, C. M.; Altable, M.; Filippone, S.; Domenech, A. M.; Martin, N.; Echegoyen, L. *Angew. Chem., Int. Ed.* **2006**, *45*, 7430−7433. (t) Rodriguez-Fortea, A.; Campanera, J. M.; Cardona, C. M.; Echegoyen, L.; Poblet, J. M. *Angew. Chem., Int. Ed.* **2006**, *45*, 8176−8180. (u) Yang, S.; Dunsch, L. *Chem.—Eur. J.* **2006**, *12*, 413−419. (v) Stevenson, S.; Mackey, M. A.; Coumbe, C. E.; Phillips, J. P.; Elliot, B.; Echegoyen, L. *J. Am. Chem. Soc.* **2007**, *129*, 6072−6073. (w) Lukoyanova, O.; Cardona, C. M.; Rivera, J.; Lugo-Morales, L. Z.; Chancellor, C. J.; Olmstead, M. M.; Rodriguez-Fortea, A.; Poblet, J. M.; Balch, A. L.; Echegoyen, L. *J. Am. Chem. Soc.* **2007**, *129*, 10423−10430.
(6) (a) Balzani, V.; Credi, A.; Raymo, F. M.; Stoddard, J. F. *Angew. Chem., Int. Ed.* **2000**, *39*, 3348−3391. (b) Molecular Machines Special Issue. *Acc. Chem. Res.* **2001**, *34*, 409−522.
(7) Yamada, M.; Nakahodo, T.; Wakahara, T.; Tsuchiya, T.; Maeda, Y.; Akasaka, T.; Kako, M.; Yoza, K.; Horn, E.; Mizorogi, N.; Kobayashi, K.; Nagase, S. *J. Am. Chem. Soc.* **2005**, *127*, 14570−14571.
(8) Wakahara, T.; Yamada, M.; Takahashi, S.; Nakahodo, T.; Tsuchiya, T.; Maeda, Y.; Akasaka, T.; Kako, M.; Yoza, K.; Horn, E.; Mizorogi, N.; Nagase, S. *Chem. Commun.* **2007**, 2680−2682.
(9) Yamada, M.; Wakahara, T.; Nakahodo, T.; Tsuchiya, T.; Maeda, Y.; Akasaka, T.; Yoza, K.; Horn, E.; Mizorogi, N.; Nagase, S. *J. Am. Chem. Soc.* **2006**, *128*, 1402−1403.
(10) Yamamoto, K.; Funasaka, T.; Takahashi, T.; Akasaka, T.; Suzuki, T.; Maruyama, Y. *J. Phys. Chem.* **1994**, *98*, 12831−12833.

***Scheme 1***

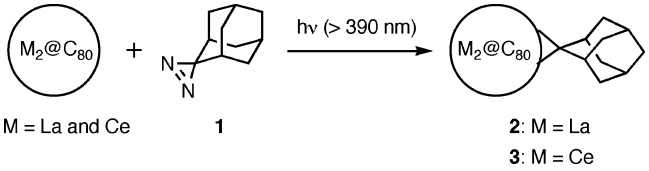


Hz, 2H), 3.59 (brs, 2H); $^{13}$C NMR (125 MHz, $C_2D_2Cl_4/CS_2$, 303 K) $\delta$ 153.5 (2C), 151.1 (2C), 150.7 (2C), 150.3 (2C), 150.1 (2C), 149.9 (1C), 149.6 (2C), 149.1 (2C), 147.8, (2C), 147.1 (2C), 146.1 (2C), 144.9 (4C), 144.0 (2C), 143.8 (2C), 143.7 (1C), 143.3 (2C), 142.8 (2C), 141.3 (1C), 141.1 (2C), 141.0 (1C), 139.9 (2C), 137.4 (2C), 137.3 (2C), 137.2 (2C), 137.1 (2C), 137.0 (2C), 137.0 (2C), 136.8 (2C), 135.2 (2C), 134.8 (1C), 134.5 (4C), 134.3.(2C), 134.0 (2C), 133.9 (2C), 132.7 (1C), 131.8 (2C), 131.4 (2C), 130.6 (2C), 125.8 (2C), 123.8 (2C), 119.9 (1C), 97.7 (1C), 46.2 (s, 1C), 37.3 (t, 1C), 35.9 (d, 2C), 34.4 (t, 2C), 34.9 (t, 2C), 27.9 (d, 1C), 27.0 (d, 1C); MALDI-TOF MS *m*/*z* 1372 [M$^-$].

Black crystals of **2**·1(ODCB)were obtained by slow evaporation of a solution of **2** in ODCB and hexane. Single-crystal X-ray diffraction data were collected on a Rigaku R-AXIS RAPID equipped with an imaging plate area detector using Mo K$\alpha$ radiation in the scan range $3.09° < \theta < 27.42°$. Crystal data of **2**·1(ODCB): $C_{96}H_{18}Cl_2La_2$, $M_W = 1519.82$, orthorhombic, space group *Pbca*, $a = 21.958(3)$ Å, $b = 22.035(2)$ Å, $c = 20.4625(17)$ Å, $\alpha = \beta = \gamma = 90.00°$, $V = 9900.8(17)$ Å$^3$, $Z = 8$, $D_{calc} = 2.039$ Mg/m$^3$, $\mu = 1.880$ mm$^{-1}$, $T = 133$ K, crystal size $0.36 \times 0.42 \times 0.18$ mm$^3$; 89 327 reflections, 11 244 unique reflections; 9220 with $I > 2\sigma(I)$; $R_1 = 0.0590$ [$I > 2\sigma(I)$], $wR_2 = 0.1680$ (all data), GOF (on $F^2$) = 1.232. The maximum residual electron density is equal to 3.918 eÅ$^{-3}$.

**Ce$_2$@C$_{80}$(Ad) (3):** $^{13}$C NMR (125 MHz, $C_2D_2Cl_4/CS_2$ = 1/3, 303 K) $\delta$ 194.2 (2C), 191.7 (2C), 186.2 (2C), 184.8 (1C), 183.9 (1C), 180.8 (2C), 172.3 (2C), 171.4 (2C), 170.3 (4C), 167.6 (2C), 167.5 (2C), 162.7 (2C), 160.0 (2C), 159.4 (4C), 158.5 (2C), 157.1 (2C), 156.1 (2C), 155.4 (2C), 153.7 (2C), 149.2 (2C), 149.1 (2C), 148.2 (2C), 146.2 (1C), 145.8 (2C), 145.3 (2C), 143.9 (2C), 142.6 (2C), 137.4 (2C), 136.8 (2C), 135.5 (1C), 133.3 (2C), 128.4 (2C), 125.1 (2C), 118.8 (2C), 104.3 (2C), 95.9 (2C), 85.4 (3C), 84.9 (3C), 41.1 (1C), 24.0 (1C or 2C), 23.0 (1C or 2C), 19.3, 18.3, 17.2 (1C), 14.8 (1C or 2C), 13.8 (1C or 2C), 4.8 (1C). MALDI-TOF MS *m*/*z* 1374 [M$^-$].

**Theoretical Calculations.** Geometries were optimized with hybrid density functional theory at the B3LYP[11] level using the Gaussian 03 program.[12] The effective core potential and the corresponding basis set were used for La, and electrons in the outermost core orbitals were explicitly treated as valence electrons.[13] The contraction schemes employed for the basis set was (5s5p3d)/[4s4p3d] for La in standard notation. The split-valence d-polarized 6-31G*[14] basis set was used for C and H.

## Results and Discussion

**Synthesis and Characterization of 2 and 3.** Irradiation of a toluene solution of M$_2$@C$_{80}$ and an excess molar amount of **1** in a degassed sealed tube at room temperature using a high-pressure mercury-arc lamp (cutoff <390 nm) resulted in the formation of the corresponding adduct, M$_2$@C$_{80}$(Ad) (**2**: M = La, **3**: M = Ce, Ad = adamantylidene), in 80% yield, which was purified by preparative HPLC, respectively (Scheme 1). The formation of **2** and **3** was confirmed by mass spectroscopic measurements. Mass spectrometry of **2** and **3** displays a parent peak at *m*/*z* 1372 ($C_{90}H_{14}La_2$) and 1374 ($C_{90}H_{14}Ce_2$), respectively.

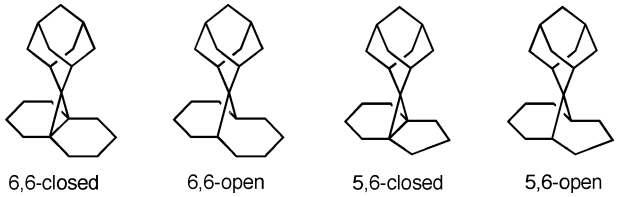


***Figure 1.*** Four addition patterns.

***Table 1.*** Four NMR Patterns of C$_{80}$(Ad) Isomers

| addition form | symmetry | $^{13}$C NMR pattern of C$_{80}$ cage: sp$^2$ | $^{13}$C NMR pattern of C$_{80}$ cage: sp$^3$ | $^{13}$C NMR pattern of Ad group | $^1$H NMR pattern of Ad group |
|---|---|---|---|---|---|
| 6,6-closed | $C_s$ | 1C × 6, 2C × 36 | 1C × 2 | 7 lines | 8 lines |
| 6,6-open | $C_s$ | 1C × 8, 2C × 36 | 0 | 7 lines | 8 lines |
| 5,6-closed | $C_s$ | 1C × 8, 2C × 35 | 2C × 1 | 7 lines | 9 lines |
| 5,6-open | $C_s$ | 1C × 8, 2C × 36 | 0 | 7 lines | 9 lines |

The $I_h$ structure of the C$_{80}$ fullerene has two kinds of nonequivalent carbon atoms. Therefore, there are two possible reaction sites for the addition of the Ad carbene on the C$_{80}$ cage. In addition, there are two possibilities of whether the bond on the addition site is cleaved or not. Therefore, four addition patterns are possible for the addition of the carbene to the C$_{80}$ cage, as shown in Figure 1.

Four NMR patterns of **2** are listed in Table 1. The $^{13}$C NMR spectrum of **2** shows 44 signals for the C$_{80}$ cage, of which 8 peaks are at half intensity and 36 peaks are at full intensity. On the other hand, no carbon signal assignable to the cyclopropane ring on the cage was observed. These results suggest that **2** has a 6,6-open structure.[15,16] In addition, the HMQC NMR of **2** shows 8 kinds of correlation between the proton and the carbon signals on the Ad skeleton. This supports the 6,6-open structure of **2**.

In the case of **3**, its low solubility and the paramagnetic effects derived from the 4f electron spin remaining on Ce atoms prohibit us from assigning the $^{13}$C signals. In order to solve these problems, $^{13}$C-enriched Ce$_2$@C$_{80}$ was used for the reaction. The $^{13}$C NMR spectrum of **3** having a $^{13}$C-enriched C$_{80}$ cage shows 44 signals assignable to the C$_{80}$ cage. Therefore, this confirms that **3** has a 6,6-open structure, as does **2**.

The vis−near-IR absorption spectra of **2** and **3** are similar to those of the pristine La$_2$@C$_{80}$ and Ce$_2$@C$_{80}$, respectively (Figure 2). These indicate that the $\pi$-electronic state of the C$_{80}$ cage is little changed by the Ad addition. This is because the sp$^2$-character of the carbon atoms at the addition site is retained. For comparison, the spectrum of a 6,6-closed isomer of La$_2$@C$_{80}$(CH$_2$)$_2$NTrt[9] is also shown in Figure 2. The La$_2$@C$_{80}$(CH$_2$)$_2$-NTrt isomer displays absorption maxima at 660 and 700 nm, unlike the featureless spectra of the carbene adducts.

(11) (a) Becke, A. D. *Phys. Rev. A* **1988**, *38*, 3098−3100. (b) Becke, A. D. *J. Chem. Phys*. **1993**, *98*, 5648−5652. (c) Lee, C.; Yang, W.; Parr, R. G. *Phys. Rev. B* **1988**, *37*, 785−789.
(12) Frisch, M. J. et al. *GAUSSIAN 03*, revision C. 01; Gaussian Inc.: Wallingford, CT, 2004.
(13) Hay, P. J.; Wadt, W. R. *J. Chem. Phys.* **1985**, *82*, 299−310.
(14) Hehre, W. J.; Ditchfield, R.; Pople, J. A. *J. Chem. Phys.* **1972**, *56*, 2257−2261.
(15) Maeda, Y. et al. *J. Am. Chem. Soc.* **2004**, *126*, 6858−6859.
(16) Iiduka, Y.; Wakahara, T.; Nakahodo, T.; Tsuchiya, T.; Sakuraba, A.; Maeda, Y.; Akasaka, T.; Yoza, K.; Horn, E.; Kato, T.; Liu, M. T. H.; Mizorogi, N.; Kobayashi, K.; Nagase, S. *J. Am. Chem. Soc.* **2005**, *127*, 12500−12501.
(17) Suzuki, T.; Maruyama, Y.; Kato, T.; Kikuchi, K.; Nakao, Y.; Achiba, Y.; Kobayashi, K.; Nagase, S. *Angew. Chem., Int. Ed. Engl.* **1995**, *34*, 1094−1096.

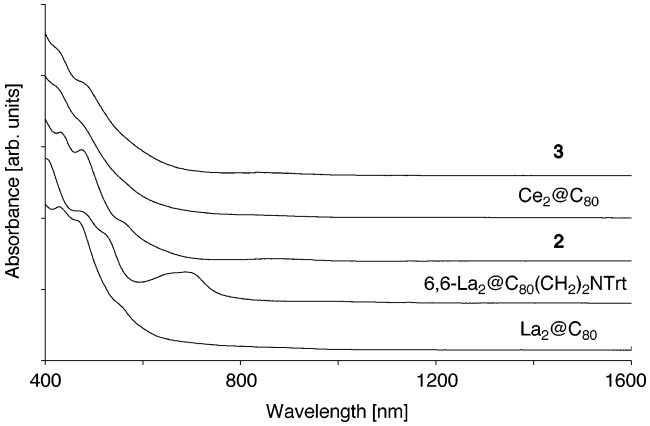


***Figure 2.*** Vis−near-IR absorption spectra of $La_2@C_{80}$, 6,6-$La_2@C_{80}(CH_2)_2$-NTrt, **2**, $Ce_2@C_{80}$, and **3** in $CS_2$ solution.

***Table 2.*** Redox Potentials[a] of **2**, **3**, and $M_2@C_{80}$ (M = La and Ce)

| compd | $^{ox}E_2$ | $^{ox}E_1$ | $^{red}E_1$ | $^{red}E_2$ | $^{red}E_3$ |
|---|---|---|---|---|---|
| **2** | +0.86[b] | +0.49 | −0.36 | −1.78 | 2.33[b] |
| $La_2@C_{80}$[d] | +0.95 | +0.56 | −0.31 | −1.71 | −2.13[c] |
| **3** | −0.89[b] | +0.47 | −0.43 | | |
| $Ce_2@C_{80}$[e] | +0.95 | +0.57 | −0.39 | −1.71 | |

[a] Half-cell potentials unless otherwise stated. Values are in volts relative to ferrocene/ferrocenium couple. [b]Values are obtained by DPV. [c]Irreversible. [d]Reference 17. [e]Reference 7.

The redox potentials of **2** and **3** were investigated by CV and DPV measurements. As shown in Table 2, the first oxidation potentials of **2** and **3** were cathodically shifted to 70 and 100 mV, and the first reduction potentials were cathodically shifted to 50 and 40 mV as compared to the pristine $La_2@C_{80}$ and $Ce_2@C_{80}$, respectively. These cathodic shifts indicate that the introduction of an Ad group results in decreasing the electron-accepting properties.[15] The small shifts of oxidation and reduction potentials reflect the fact that the HOMO−LUMO gaps of **2** and **3** resemble those of the pristine $La_2@C_{80}$ and $Ce_2@C_{80}$, respectively. This suggests that the conjugated character of the fullerene cage is only slightly changed despite the C−C bond cleavage due to the carbene addition.

**X-ray Crystallographic Analysis of 2.** The detailed structure of **2** was revealed by single-crystal X-ray structure analysis. The crystal structure shown in Figure 3 confirms the 6,6-open structure of **2**. The opened C−C separation is 2.166 Å, whereas the 6,6-bond length on the addition site of 6,6-$La_2@C_{80}(CH_2)_2$-NTrt[9] is 1.635 Å. The 6,6-bond cleavage results in the protrusion of the carbon atoms on the cage and the expansion of the inner space of the cage. Very recently, Echegoyen and co-workers have also reported a similar 6,6-open structure for a $Y_3N@C_{80}$ adduct.[5w]

It is interesting that the two La atoms in **2** are collinear with the spiro carbon of the 6,6-open adduct. The metal positions are quite different from those in 6,6-$La_2@C_{80}(CH_2)_2$NTrt,[9] $Ce_2@C_{80}(Mes_2Si)_2CH_2$,[7] and $La_2@C_{80}(Ar_2Si)_2CH_2$ (Ar = Mes and Dep).[8] As Figure 3 shows, the La1 atom far from the Ad group is located with La1−C65 = 2.587 Å, La1−C73 = 2.430 Å, La1−C74 = 2.424 Å, and La1−C80 = 2.648 Å. The La2 atom near Ad is located with La2−C1 = 2.630 Å, La2−C13 = 2.577 Å, La2−C3 = 2.618 Å, and La2−C2 = 2.594 Å. Furthermore, it is noteworthy that the La−La distance is highly elongated to 4.031 Å. For comparison, the La−La distance in $La_2@C_{80}$ and its derivatives are listed in Table 3. Unfortunately,

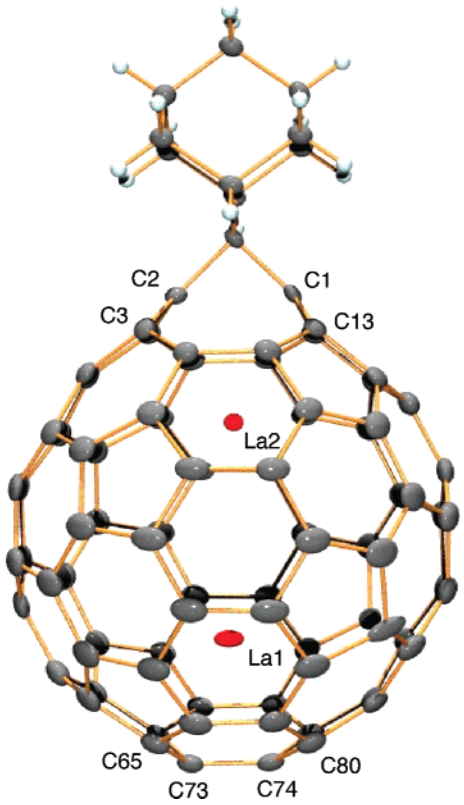


***Figure 3.*** ORTEP drawing of **2** showing thermal ellipsoids at the 50% probability level at 133 K. The ODCB molecule is omitted for clarity. Only one La site with the highest occupancy (0.99) is shown.

***Table 3.*** La−La Distances (in Å) of $La_2@C_{80}$ and Its Derivatives

| compound | La–La distance [Å] | method |
|---|---|---|
| **2** | 4.031 | single-crystal X-ray |
| 6,6-$La_2@C_{80}(CH_2)_2$NTrt[a] | 3.823 | single-crystal X-ray |
| $La_2@C_{80}(Dep_2Si)_2CH_2$[b] | 3.792 | single-crystal X-ray |
| $La_2@C_{80}$[c] | 3.87−3.90 | XAFS |
| $La_2@C_{80}$[d] | 3.84 | powder X-ray (MEM/Rietveld) |
| $La_2@C_{80}$ ($D_{2h}$)[e] | 3.655 | HF calculation |
| $La_2@C_{80}$ ($D_{2h}$)[c] | 3.735 | DFT calculation (B3LYP/6-31G*) |
| $La_2@C_{80}$ ($D_{3d}$)[f] | 3.731 | DFT calculation (B3LYP/DZP) |
| $La_2@C_{80}$ ($D_{2h}$)[g] | 3.828 | DFT calculation (ZRDTZP) |

[a] Reference 9. [b]Reference 8. [c]Reference 18. [d]Reference 3c. [e]Reference 4a. [f]Reference 3d. [g]Reference 19.

the La−La distance in $La_2@C_{80}$ has not been determined by single-crystal X-ray structure analysis. In 1995, we carried out theoretical calculations for $La_2@C_{80}$ and predicted that the most stable structure has $D_{2h}$ symmetry.[4a] The La−La distance was calculated to be 3.655 (HF)[4a] and 3.735 (B3LYP) Å,[18] the latter value being closer to those of 3.87−3.90 Å determined by the La K-edge XAFS method.[18] Recently, Shimotani and co-workers have claimed that the $D_{3d}$ structure is slightly more stable than the $D_{2h}$ structure and the La−La distance is 3.731 Å.[3d] However, Hao and co-workers have very recently confirmed with ZORA (zero-order regular approximation) methods that the $D_{2h}$ structure is the most stable for $La_2@C_{80}$, as predicted by us in 1995,[4a] and calculated that the La−La distance is 3.828 Å.[19] As

(18) Kubozono, Y.; Takabayashi, Y.; Kashino, S.; Kondo, M.; Wakahara, T.; Akasaka, T.; Kobayashi, K.; Nagase, S.; Emura, S.; Yamamoto, K. *Chem. Phys. Lett.* **2001**, *335*, 163−169.

***Table 4.*** Anisotropic Temperature Factors of Lanthanum and Carbon Atoms at 103, 133, 188, and 273 K of **2**

| | La1 | La2 | C (cage)[a] |
|---|---|---|---|
| 103 K | 0.012 | 0.027 | 0.021 |
| 133 K | 0.014 | 0.032 | 0.024 |
| 188 K | 0.016 | 0.041 | 0.028 |
| 273 K | 0.021 | 0.058 | 0.044 |

[a] Average value for the carbon atoms of the fullerene cage.

summarized in Table 3, the single-crystal X-ray structure analyses of 6,6-$La_2$@$C_{80}(CH_2)_2$NTrt and $La_2$@$C_{80}(Dep_2Si)_2CH_2$ show that the La−La distances are similar to those of $La_2$@$C_{80}$. In contrast, it is notable that the La−La distance in **2** is ca. 0.2−0.3 Å longer than that in $La_2$@$C_{80}$. It is suggested that the remarkable La−La elongation in **2** is due to the expansion of the inner space of the cage caused by the bond cleavage, which reduces the electrostatic repulsion between the positively charged La atoms.

To clarify the motion of the La atoms in crystal, single-crystal X-ray structure analyses were carried out by varying temperatures. Table 4 shows the anisotropic temperature factors of La and carbon atoms at 103, 133, 188, and 273 K. The linear increase with increasing temperature was observed for La1, La2, and carbon atoms. The anisotropic temperature factors of the La atoms are similar to those of the cage carbon atoms, indicating that the La atoms rather stand still in the crystal structure. In addition, the anisotropic temperature factors of La2 are almost twice as large as those of La1, suggesting that La1 is more static than La2.

In an attempt to characterize the Ce positions in **3** by single-crystal X-ray structure analysis, crystallization was not successful. However, it is expected that the metal positions in **3** resemble those in **2** because of the similarity in metal positions between $La_2$@$C_{80}(Dep_2Si)_2CH_2$[8] and $Ce_2$@$C_{80}(Mes_2Si)_2CH_2$[7] found by the single-crystal X-ray structure analyses.

**Paramagnetic $^{13}$C NMR Spectral Analysis of 3.** The dynamic behavior of the Ce atoms in **3** was investigated by means of paramagnetic $^{13}$C NMR spectral analysis. The $^{13}$C NMR chemical shifts ($\delta$) of **3** exhibit temperature-dependent shifts that originate from the buried f-electron spin remaining on the $Ce^{3+}$ ($4f^15d^06s^0$) atoms (Figure 4).

The chemical shifts of paramagnetic molecules in solutions are generally expressed as a sum of three contributions from diamagnetic ($\delta_{dia}$), Fermi contact ($\delta_{fc}$), and pseudocontact ($\delta_{pc}$) shifts where the paramagnetic $\delta_{fc}$ and $\delta_{pc}$ are proportional to $T^{-1}$ and $T^{-2}$ ($T$ = absolute temperature), respectively (eq 1).[20]

$$\delta = \delta_{dia} + \delta_{fc} + \delta_{pc} \quad (1)$$

The $\delta_{dia}$ values correspond to the $^{13}$C chemical shifts of the diamagnetic **2**. $^{13}$C enrichment of the fullerene cage enabled us to observe the $^{13}$C NMR shifts of **3**, despite the low solubility. As clearly shown in Figure S9, the values at $T^{-1} = 0$ extrapolated by the line-fitting plot with $T^{-1}$, which correspond to the $\delta_{dia}$ values of **3**, deviate significantly from the observed $^{13}$C chemical shifts of **2**. On the other hand, the values at $T^{-2} = 0$ on the line-fitting plot with $T^{-2}$ are in good agreement with the observed $^{13}$C chemical shifts of **2**, as shown in Figure S10. These suggest that $\delta_{pc}$ makes a much larger contribution than $\delta_{fc}$ for the chemical shifts of **3**, as is apparent from the fact that there is no significant connection between the Ce atoms and cage carbons.[5n,7,21] The carbon signals due to the sp$^2$-carbon atoms on the addition position of the cage and the spiro carbon on the Ad group were assigned based on the agreement between the extrapolated values at $T^{-2} = 0$ by the line-fitting plot with $T^{-2}$ and the chemical shifts of **2**. The $\delta_{pc}$ of **3** is briefly written in the following equation (eq 2)

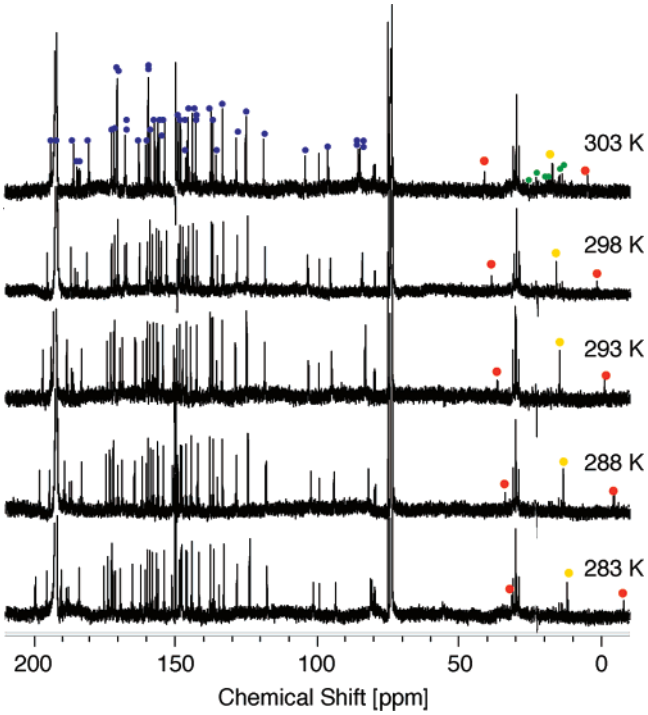


***Figure 4.*** $^{13}$C NMR spectra of **3** at 283−303 K. The signals marked by blue, red, orange, and green solid circles are due to the sp$^2$ carbon atoms on the cage, sp$^2$ carbon atoms on the addition position of the cage, spiro carbon on the Ad group, and the other carbon atoms on the Ad group, respectively.

$$\delta_{pc} = \frac{C(3\cos^2\theta - 1)}{r^3T^2} \quad (2)$$

where $r$ is the distance between Ce and cage carbons, $\theta$ is the angle between the $r$ vector and the vertical axis on which the two Ce atoms locate, and $C$ is a common constant with a negative value for all cage carbons. Figure 5 shows the temperature dependence for $T^{-2}$, i.e., $C(3\cos^2\theta - 1)/r^3$, for each carbon signal of **3**.

The sp$^2$ carbon signals on the $C_{80}$ cage of **3** are highly shifted compared to those of the pristine $Ce_2$@$C_{80}$[7] upon decreasing the temperature from 303 to 283 K. This can be explained by the fact that the motion of two Ce atoms in **3** is fixed at specific positions, just like the case of $Ce_2$@$C_{80}(Mes_2Si)_2CH_2$.[7] In addition, the sp$^2$ carbon signals on the addition position and the spiro carbon on the Ad group show particularly highly negative values. This indicates that the positions of two Ce atoms

(19) Zhang, J.; Hao, C.; Li, S.; Mi, W.; Jin, P. *J. Phys. Chem. C* **2007**, *111*, 7862−7867.
(20) Bleaney, B. *J. Magn. Reson.* **1972**, *8*, 91−100.
(21) (a) Wakahara, T.; Kobayashi, J.; Yamada, M.; Maeda, Y.; Tsuchiya, T.; Okamura, M.; Akasaka, T.; Waelchli, M.; Kobayashi, K.; Nagase, S.; Kato, T.; Kako, M.; Yamamoto, K.; Kadish, K. M. *J. Am. Chem. Soc.* **2004**, *126*, 4883−4887. (b) Yamada, M.; Wakahara, T.; Lian, Y.; Tsuchiya, T.; Akasaka, T.; Waelchli, M.; Mizorogi, N.; Nagase, S.; Kadish, K. M. *J. Am. Chem. Soc.* **2006**, *128*, 1400−1401.

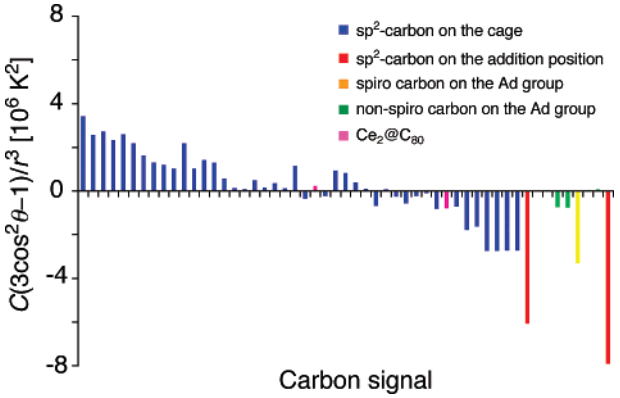


***Figure 5.*** Temperature dependence for $T^{-2}$ of **3**. Carbon signal lines in order of chemical shifts at 303 K.

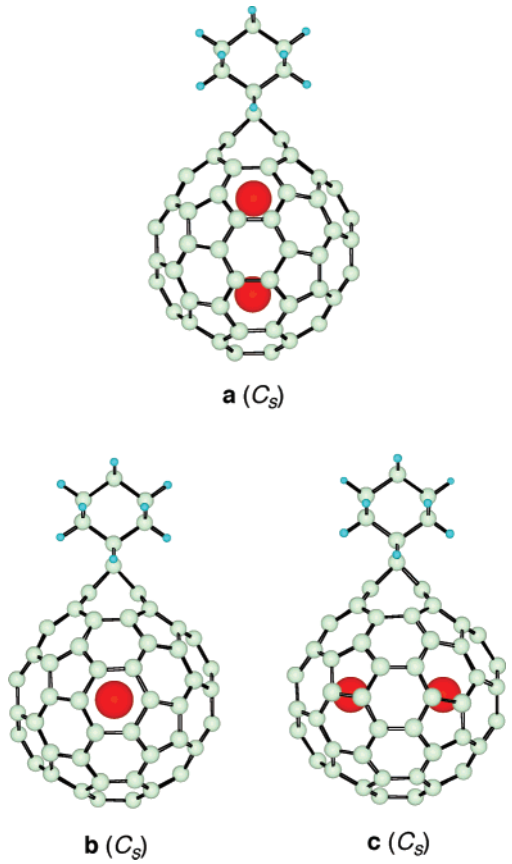


***Figure 6.*** Structures of **2** optimized by changing the positions of the La atoms.

in **3** differ little from those of the La atoms in **2**. Therefore, the Ce positions are also regulated at room temperature in solution, as in the La case.

**Theoretical Calculations.** As already mentioned, the positively charged metal atoms are highly stabilized at the minimum of electrostatic potentials inside the fullerene cage. The electronic structure of $M_2@C_{80}$(Ad) is formally described as $[M_2]^{6+}[C_{80}(Ad)]^{6-}$. The electrostatic potentials inside $[C_{80}(Ad)]^{6-}$ were calculated. The electrostatic potential map shows a minimum near the bottom of the cage (i.e, near the La1 atom in Figure 3). Two metal atoms should be most highly stabilized when one metal atom is located near the minimum and the other metal atom is far away to minimize the electrostatic repulsion between the positively charged metal atoms (see Figure S11 in Supporting Information). As a result, the two metal atoms are located, as shown in Figure 3. This was also confirmed by optimizing the structure of **2** using density functional calculations (Figure 6a). Figure 6 also shows the structures optimized by changing the positions of the La atoms. The relative energies and La−La distances are listed in Table 5.

***Table 5.*** Relative Energies for the Optimized Structures of **2**

| sturcture | symmetry | La–La distance [Å] | relative energy [kcal/mol] |
|---|---|---|---|
| **a** | $C_s$ | 3.891 | 0.0 |
| **b** | $C_s$ | 3.669 | 22.2 |
| **c** | $C_s$ | 3.739 | 31.2 |

It is apparent from Table 5 that structure **a** is the most stable and agrees with the X-ray crystal structure in Figure 3. On the other hand, structures **b** and **c** are 22.2 and 31.2 kcal/mol less stable than structure **a**, respectively, confirming that the circular rotation of two La atoms is considerably hindered. It is also to be noted that the longest La−La distance is achieved in **a**, which contributes to the stabilization of **a** because of the decrease in the electrostatic repulsion between the two La atoms.

The HOMO and LUMO levels of **2** (structure **a**) were calculated to be −5.23 eV and −3.88 eV, respectively. On the other hand, the HOMO and LUMO levels of $La_2@C_{80}$ are −5.40 eV and −4.21 eV, respectively.[22] The HOMO−LUMO gap of **2** (1.35 eV) is slightly larger than that of $La_2@C_{80}$ (1.19 eV). This agrees well with the CV and DPV results.

## Conclusions

The selective addition of the adamantylidene carbene occurs at the 6,6-junction of the $M_2@C_{80}$ with the bond cleavage to afford the formation of the 6,6-open adduct, $M_2@C_{80}$(Ad). The structures of adducts **2** (M = La) and **3** (M = Ce) were characterized by means of NMR spectroscopy and X-ray crystallographic analysis. Crystallographic data for **2** reveals that the two La atoms are collinear with the spiro carbon of the adduct with a long La−La distance, unlike the three-dimensional random motion in $La_2@C_{80}$. The unique La positions are confirmed by density functional calculations. Paramagnetic $^{13}$C NMR spectral analysis of **3** indicates that the positions of the Ce atoms are also regulated at room temperature in solution, in the same way found for **2**.

**Acknowledgment.** M.Y. thanks the Japan Society for the Promotion of Science (JSPS) for the Research Fellowship for Young Scientists. This work was supported in part by a Grant-in-Aid, the 21st Century COE Program, Nanotechnology Support Project, The Next Generation Super Computing Project (Nanoscience Project), and Scientific Research on Priority Area from the Ministry of Education, Culture, Sports, Science, and Technology of Japan, and a grant from the Kurata Memorial Hitachi Science and Technology Foundation.

**Supporting Information Available:** Crystallographic data in CIF format, the complete list of authors for refs 12 and 15, spectroscopic data for **2** and **3**, and the total energies (hartree) and Cartesian coordinates (Å) of $La_2@C_{80}$(Ad). This material is available free of charge via the Internet at http://pubs.acs.org.

JA073924W

(22) (a) Suzuki, T.; Maruyama, Y.; Kato, T.; Kikuchi, K.; Nakao, Y.; Achiba, Y.; Kobayashi, K.; Nagase, S. *J. Am. Chem. Soc.* **1995**, *34*, 1094−1096. (b) Iiduka, Y.; Ikenaga, O.; Sakuraba, A.; Wakahara, A.; Tsuchiya, T.; Maeda, Y.; Nakahodo, T.; Akasaka, T.; Kato, M.; Mizorogi, N.; Nagase, S. *J. Am. Chem. Soc.* **2005**, *127*, 9956−9957.